Contents lists available at SciOpen

Food Science and Human Wellness

journal homepage: https://www.sciopen.com/journal/2097-0765

China Food Publishing Co.

Characterization of high intensity ultrasound on structure, digestibility, and IgG binding capacity of Pacific oyster (*Crassostrea gigas*) tropomyosin

Li Liu[a], Xue Liu[a], Yuyang Ma[a], Mingyong Zeng[a,b,*]

[a] College of Food Science and Engineering, Ocean University of China, Qingdao 266003, China
[b] Qingdao Engineering Research Center for Preservation Technology of Marine Foods, Qingdao 266003, China

ARTICLE INFO

Article history:
Received 26 March 2024
Received in revised form 30 April 2024
Accepted 9 August 2024

Keywords:
Crassostrea gigas
High intensity ultrasound
Tropomyosin
Protein structure
Digestibility
IgG binding capacity

ABSTRACT

In this study, the different powers (100−500 W) of high intensity ultrasound (HIU) were configured to investigate the mechanism of action on the tropomyosin (TM) structure, immunoglobulin G (IgG) binding capacity and digestive properties in oyster. The α-helix content of the HIU-treated TM decreased from 75.3% (control) to 41.8% (500 W) with the conversion of α-helix to random coil in TM molecules. The tertiary structure was changed with the decrease of particle size (from 165.5 to 85.6 nm) and the variety in aggregation state. Remarkably, the IgG binding capacity of TM decreased resulting from the higher power HIU treatment (300−500 W). After gastrointestinal digestion, the binding capacity of TM to IgG decreased to 1.31 with 500 W treatment, while the digestibility significantly increased. Overall, the present study suggested that the HIU-induced structural changes contributed to improving *in vitro* digestibility and reducing IgG binding capacity. This study contributes significant potential in terms of oyster allergen reduction.

1. Introduction

Food allergens are usually proteins with molecular weights in the range of 10−70 kDa, which has a serious threat to human health and safety with the worldwide attention[1]. As a high quality protein resource, oyster is widely consumed around the world by fresh food and processed into various products because of the unique flavor and nutrition. According to clinical studies, oyster consumption can trigger a range of allergic reactions including vomiting, edema, dizziness, hives, breathing difficulties and even life threatening[2]. Tropomyosin (TM) is a major allergen in shellfish and possess a typical coiled-coil structure formed by 2 parallel α-helices with a molecular weight of about 38 kDa[3]. Until now, the only way to avoid oyster allergy is to avoid eating. Previous studies have shown that allergic patients have an immune response to TM that binds to crab-specific immunoglobulin E (IgE) in these patients[4]. Therefore, reduction the antigenicity of TM is beneficial to oyster-allergic individuals. There is a necessity for effective methods to reduce or eliminate the allergenicity of oysters.

The subduction of allergenicity in process is one of the effective strategies to control food allergy. It is possible for some process techniques to denature proteins in foods, including allergens, thereby reducing the allergenicity of foods. TM has thermal stability and more epitopes can expose or form at high temperature, resulting in the increase of allergenicity[5]. Thus, conventional thermal processing is not effective in reducing the allergenicity of oysters. Compared with chemical methods (acid or metal ion treatment) and biological methods (enzymatic digestion or fermentation), the emerging physical treatment technology, especially high intensity ultrasound (HIU) has become the most common method to eliminate allergen[6]. HIU is a residue free and low-cost technology that also preserves the original

* Corresponding authors at: College of Food Science and Engineering, Ocean University of China, Qingdao 266003, China.
Email address: mingyz@ouc.edu.cn (M.Y. Zeng)
Peer review under responsibility of Beijing Academy of Food Sciences.

SciOpen Publishing services by Tsinghua University Press

http://doi.org/10.26599/FSHW.2024.9250366

flavor and quality of food to the maximum extent. However, there is a gap in research on the effects of HIU on oyster TM and sensitization reduction.

Ultrasound can create bubbles or cavities in the fluid and the process of bubble growth and implosion is called cavitation. This process releases energy and generates strong turbulence and shear stress in the cavitation zone[7]. Moreover, the process accompanied by several special effects, such as momentary extreme temperature hotspots (approximately 5 500 °C), high pressure shocks (approximately 1 000 bar), high speed microjets (100 m/s), shock waves, acoustic flow, and free radicals generated from dissociated water molecules[8]. These combined effects can lead to the changes of food allergenicity by affecting the structure of allergic proteins. The HIU (20−100 kHz, > 1 W/cm^2) was effective in reducing food allergenicity. Previous studies have shown that ultrasonic treatment can be used to reduce food sensitization. Dong et al.[9] reported as the duration of the HIU (20 kHz, 400 W) increased, the shrimp sensitization decreased with an optimal treatment time of 20 min. Besides, Chen et al.[10] illustrated that the allergenicity of shrimp decreased with increasing ultrasound power. Hussain et al.[11] suggested that HIU (25 kHz, 900 W, 60 min) could be used to produce hypoallergenic milk, which resulted in small diameter (< 100 nm) of colloidal casein. However, Kerezsi et al.[12] showed that HIU (500 W) treatment was not effective in reducing the major allergens of milk. The reduction of food allergenicity by ultrasound treatment was probably related to the intensity and duration of process. Additionally, the effect of HIU treatment on the structural changes and property characterization of oyster TM has rarely been reported.

Therefore, the objectives of this study were to investigate the effects of HIU treatment on the primary and secondary structure and hydrophobicity of the oyster TM; alterations of *in vitro* digestive properties; variations in the ability to bind to IgG. Moreover, an attempt was made to reveal possible mechanisms of HIU treatment to reduce the TM of oyster allergenicity. This work provides a theoretical reference for the development of hypoallergenic shellfish products using HIU technology.

2. Materials and methods

2.1 Chemical reagents and sample preparation

Fresh oysters (*Crassostrea gigas*) were acquired from Qingdao aquatic markets and transported to the laboratory on ice. Oyster specifications were as follows: shell length 48−50 mm, shell width 27−30 mm, shell height 85−100 mm, weight 65−90 g. The pepsin (3 000 U/g) and trypsin (250 U/g) was obtained from Solarbio Technology Co., Ltd. (Beijing, China). 3,3′,5,5′-Tetrmethylbenzidine (TMB) and bromophenol blue (BPB) and was got from Sigma Aldrich Co., Ltd. (Shanghai, China). BCA Protein Assay Kit and HRP-labeled Goat Anti-Rabbit IgG (H+L) were purchased from Beyotime Technology Co., Ltd. (Shanghai, China). All other chemical reagents were analytical grade purchased from Beijing Reagent Co., Ltd. (Beijing, China).

2.2 Preparation of oyster TM

The preparation of TM was carried out as described with some modifications[13-14]. The muscle tissue was crushed and then homogenized with phosphate buffered saline (PBS) (0.05 mol/L, pH 7) at the ratio of 1:4 (*m/V*) by a high-speed homogenizer (D-500, Wiggens Co., Ltd., Straubenhardt, Germany) for 1 min. The mixture was centrifuged at 10 000 × *g* for 15 min. The precipitate was resuspended in the above buffer and the steps were repeated twice to effectively remove sarcoplasmic proteins. The obtained precipitate was resuspended in 0.05 mol/L PBS (pH 7, 1:4, *m/V*) with 1 mol/L NaCl and extracted at 4 °C overnight. The resuspended liquid was centrifuged at 10 000 × *g* for 15 min. The supernatant was fractionated with 40% and 50% saturated $(NH_4)_2SO_4$ solution, respectively. The precipitates were dissolved and dialyzed before being heated in a 100 ℃ water bath for 10 min. Finally, all samples were stored at −20 °C for later use.

2.3 Rabbit anti-sera

The prepared TM was injected into New Zealand rabbits to obtain rabbit antisera as reported[15]. The first immunization was performed by Freund complete adjuvant mixed with immunogen (1:1, *V/V*). Freund Incomplete Adjuvant was used to perform subsequent injections at the same concentration and volume for re-stimulation every 2 weeks for a total of 4 times. Rabbit serum was centrifuged at 4 000 × *g* for 10 min (4 °C) after the titre of the indirect ELISA had reached a stable level.

2.4 HIU treatment condition

HIU treatment was performed using an ultrasonic homogenizer (JY92-IIDN, Ningbo Scientific Biotechnology Co., Ltd., China). The operating frequency is 20 kHz, and the diameter of the probe is 10 mm. TM solutions (1 mg/mL, 300 mL) were treated at various power levels (100, 200, 300, 400, 500 W) for 20 min (5 s of work and 5 s of pause). The sample without ultrasound treatment were used as control. All samples were freeze-dried to powder for further analysis by a freeze dryer (SCIENTZ-10ND, Scientz Biotechnology Co., Ltd., Zhejiang Province, China).

2.5 SDS-PAGE detection of TM

The separation (10%) and concentration gels (5%) were selected for SDS-PAGE determination according to Liu et al.[16]. Each gel lane was loaded with 10 μL of samples (1 mg/mL). The electrophoresis conditions were 30 min at 80 V and then at 120 V for 60 min. Coomassie brilliant was used for gel staining for 1 h, followed by destaining 3 times and overnight.

2.6 Fourier transform infrared spectroscopy (FTIR)

A FTIR spectrometer was used to scan FTIR spectrum of oyster TM from 4 000 to 400 cm^{-1} (Nicolet iS10, Thermo Fisher Scientific, Madison, WI, USA). The TMs of different HIU treatments was mixed with KBr (1:100) to detect the secondary structure with amide I region (1 600−1 700 cm^{-1}). The secondary structure content of the sample was calculated by PeakFit 4.12 software.

2.7 Surface hydrophobicity measurement

A volume of 80 μL of BPB (1 mg/mL) was added to 2 mL of TM solution (1 mg/mL, dissolved in PBS). The mixture was stirred at 25 °C

for 10 min at 250 r/min followed by centrifugation at 2 000 × *g* for 10 min. The supernatant was obtained by measuring the absorbance at 595 nm. Control values were obtained by examination with PBS. The binding capacity of BPB was as follows:

$$\text{Binding BPB (μg)} = \frac{80\ \mu g \times (OD_{control} - OD_{sample})}{OD_{control}} \quad (1)$$

2.8 Sulfhydryl group content of treated TM

The sulfhydryl (SH) content of TM with different HIU treatments was detected according to the previous method[17]. TM (15 mg) dissolved in Tris-glycine buffer (5 mL) was mixed with 50 μL of Ellman's reagent (4 mg/mL). The mixture was incubated at 40 °C for 25 min and centrifuged (5 000 × *g*, 15 min). The absorbance of the supernatant was measured at 412 nm with Tris-glycine buffer containing Ellman's reagent as a blank control. The SH content was calculated according to the following formula:

$$\text{SH (μmol/g)} = \frac{73.53 \times A_{412\ nm} \times D}{C} \quad (2)$$

Where, *A* was the absorbance value of the sample after removing the reagent blank; *D* was the number of dilutions; *C* represented the concentration of the sample (mg/mL).

2.9 Intrinsic fluorescence spectra measurement

The intrinsic fluorescence spectra of TM (1 mg/mL) with different HIU treatments was recorded at 295 nm by a F-4600 fluorescence spectrophotometer (Hitachi, Kyoto, Japan). The scanning range was from 300 to 400 nm with the excitation and emission slit widths of 5 nm.

2.10 UV spectra measurement

A spectrophotometer was used to detected the UV spectrum of different HIU treated TM (UV-2550, Shimadzu, Tokyo, Japan). The spectrum data were collected from 200 to 400 nm at a 0.2 nm interval.

2.11 Particle size measurement

The particle size of the TM samples was determined using a laser particle size analyzer (Malvern Nano ZS, Malvern Instruments Ltd., Worcestershire, UK). The concentrations of raw and treated TM solutions were adjusted to 1 mg/mL with 0.02 mol/L PBS (pH 7) and then filtered with a 0.22 μm filter membrane. A total of 1 mL of the solution was injected into clear test cells for analysis.

2.12 Detection of atomic force microscopy (AFM)

The morphology of the TM with different HIU treatment was observed with an AFM (SPM-9700; Shimadzu Corporation, Kyoto, Japan)[18]. The lyophilized TM samples were dispersed in distilled water (0.3 mg/mL). The 10 μL dispersion was deposited on a mica plate and dried at room temperature for 2 h. Flat and stereoscopic images were observed using a NanoScope analysis system (Bruker, USA).

2.13 In vitro digestion of TM with different HIU treatment

The *in vitro* digestion of TM with different HIU treatment was based on a previous report with some modifications[19]. The TM was blended with pepsin (400 U/mg pro) which was dissolved in 1 mL NaCl (2 mg/mL, pH 1.2). Digestion was performed at 37 °C and the pepsin was added into samples. The reaction solution was transferred to microcentrifuge tube at 0, 5, 10, 30, 60, and 90 min, respectively, finally stopped with 0.2 mol/L Na_2CO_3.

After gastric digestion, the pH of reaction solution was adjusted to 7.5 and then digested with trypsin (250 U/mg pro) at 37 °C. The trypsin was added to TM samples at about 1:200 (*m*/*m*). The reaction solution was transferred to microcentrifuge tube and immediately boiled for 5 min to terminate the reaction at 2, 5, 10, 30 and 60 min, respectively. Furthermore, the simulated digestion products were analyzed by SDS-PAGE and indirect ELISA.

2.14 Western blotting analysis

The binding ability of TM to IgG with different HIU treatments was evaluated by immunoblotting (Western blotting. PVDF membrane (0.45 μm, Wuhan Safeway Biotechnology Co., Ltd., China) was used to transfer TM bands on SDS-PAGE gels. The transfer was accomplished by using Tris-glycine buffer system at 200 mA for 70 min. The PVDF membrane was then immersed in rabbit antiserum (1:20 000 dilution) and incubated at 4 °C overnight. Subsequently, the membrane was incubated with HRP-conjugated goat anti-rabbit IgG (1:10 000 dilution) for 1 h at 25 °C. Finally, the immunoassay was photographed using a gel rapid documentation apparatus (Tanon-5200, Tanon Science & Technology Co., Shanghai, China) with ECL substrate after being washed extensively with TBST (0.01 mol/L TBS; 1% Tween-20, pH 7.4).

2.15 Dot blotting analysis

The binding capacity of TM to IgG was further investigated using dot blot analysis according to the description[20]. In brief, samples (3 μL, 0.5 mg/mL) were spotted onto nitrocellulose (NC) membranes (Servicebio Technology Co., Ltd., Wuhan, China) and incubated with rapid blocking buffer (Epizyme Biotech., Shanghai, China) for 15 min at 37 °C. The membranes were incubated with rabbit anti-sera (1:20 000 dilution) at 37 °C for 1 h. After that, the membranes were incubated with HRP-conjugated goat anti-rabbit IgG (1:10 000 dilution) at 37 °C for 1 h. Finally, the immunoassay was photographed using a gel rapid documentation apparatus (Tanon-5200, Tanon Science & Technology Co., Shanghai, China) with ECL substrate.

2.16 Indirect ELISA analysis

The binding capacity of oyster TM to IgG was further evaluated. TM was dissolved in carbonate buffer (0.05 mol/L, pH 9.6) to a final concentration of 50 μg/mL. The above solution was incorporated into a 96-well ELISA plate and incubated at 4 °C overnight. After 3 washes with TBST, blocking buffer was added to the per plate and incubated at 37 °C for 2 h. Afterwards, TMB was added to the incubated 96-well plates for 5 min at 37 °C in the dark. Finally, H_2SO_4 (2 mol/L) was moved into 96-well plates to terminate the reaction. Data were obtained by measuring absorbance at 450 nm.

2.17 Statistical analysis

All values were presented as mean ± standard deviation (SD) of triplicate measurements and analyzed using ANOVA and Duncan's multiple range tests (SPSS 22.0 software, SPSS Inc., Chicago, IL, USA) with a significance level of 0.05 ($P < 0.05$).

3. Results and discussion

3.1 SDS-PAGE analysis

As shown in Fig. 1, both natural and HIU-treated TM bands were located at around 38 kDa. Even at the maximum ultrasonic power of 500 W, the band intensity of TM remained almost parallel. However, compared with control, the electrophoretic band intensities of the TM with HIU treatment were greater, which resulted from that the higher solubility of the HIU treated TM. In previous studies, the molecular weight spectrum of squid mantle protein and grass pea protein had no change after HIU treatment[20]. Tammineedi et al.[21] reported that α-casein treated with HIU showed no significant change in protein band intensity by SDS-PAGE. These results indicated that TM could maintain the structural integrity in HIU treatment.

3.2 FTIR

The FTIR spectroscopy is a common method for assessing changes in the secondary structure of proteins. As displayed in Fig. 2, the secondary structure in the natural TM was mainly α-helix (75.3%). With the HIU treatment, the α-helix content of TM was decreased from 75.3% (control) to 41.8% (500 W). In contrast, the contents of β-turn, β-sheet, and random coil exhibited increased trends (from 7.5% to 14.8%, 6.5% to 14.0%, and 10.7% to 29.4%, respectively). These results suggested that HIU mainly induced the conversion of α-helix to random coil in TM molecules. However, the secondary structure of TM is basically unchanged with the low ultrasonic power (100 W), indicating that ultrasonic power is closely related to the structure. The hydrogen bonds of protein molecule were the main maintenance role for α-helix structures[22]. The higher ultrasonic power and the stronger cavitation facilitated the breakage of non-covalent bonds and induced the rearrangement of the protein secondary structure. The α-helix may be critical in IgG binding activity and digestibility[23-24], as it can significantly affect the structure of the protein, leading to altered IgG binding epitopes, and protease cleavage sites. The above structural modifications of proteins during HIU to form new intramolecular or intermolecular crosslinks were responsible for secondary structure changes. Therefore, alteration of hydrophobic surfaces that potentially carried IgG-binding epitopes could lead to changes in their immunoreactivity. Besides, the secondary structure rearrangement of TM might lead to significant changes in the tertiary structure.

3.3 Surface hydrophobicity of TM treated with HIU

Variations in the tertiary structure of proteins can be reflected by surface hydrophobicity, based on the degree of exposure of hydrophobic groups. As depicted in Fig. 3C, the surface hydrophobicity of HIU treated TM was significantly ($P < 0.05$) enhanced compared to the control. This indicated that HIU treatment induced protein unfolding and caused the initial buried internal hydrophobic groups to be exposed to the surface. In previous study, the enhancement of surface hydrophobicity of oyster protein[25] and chicken actomyosin by ultrasound treatment were reported.

3.4 SH group content

The SH content can partly reveal the changes in the tertiary structure of proteins. Compared to the control group (Fig. 3D), the SH content significantly ($P < 0.05$) increased with 100−300 W and exhibited a downward trend when the ultrasound power was greater than 300 W. Noticeably, the content reached (18.09 ± 0.39) μmoL/g pro in the TM samples treated at 500 W. The increase in SH content was attributed

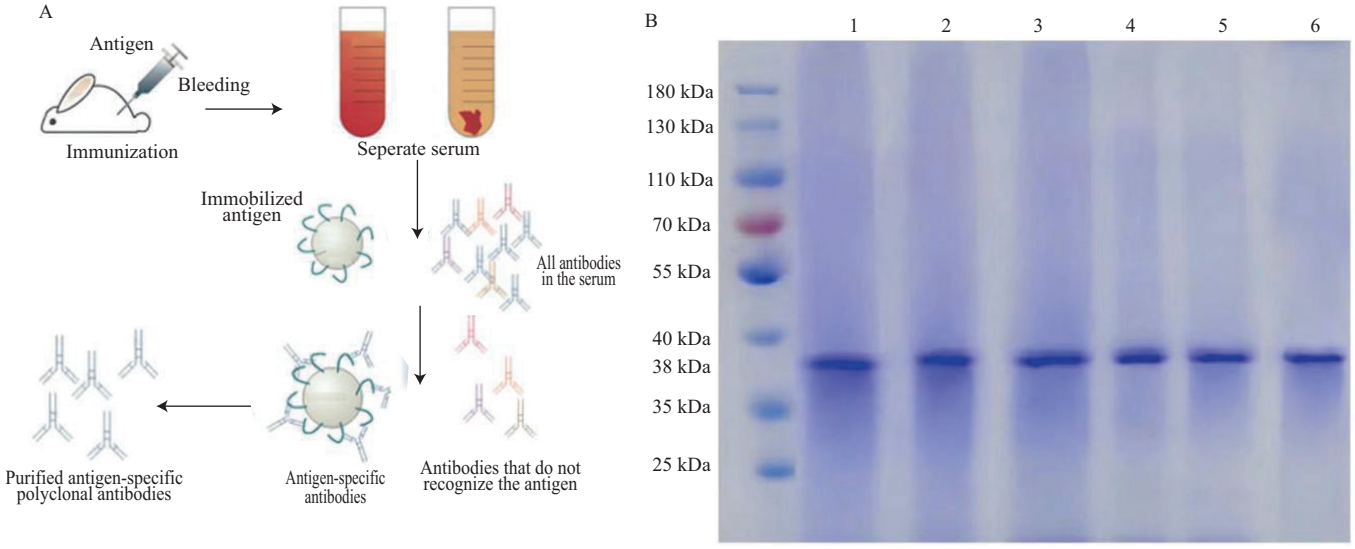

Fig. 1 Purified antigen-specific polyclonal antibodies (A) and SDS-PAGE of control and HIU treated TM (B). Lane M: marker; lane 1: control; lanes 2–6: TM treated with 100, 200, 300, 400, and 500 W, respectively.

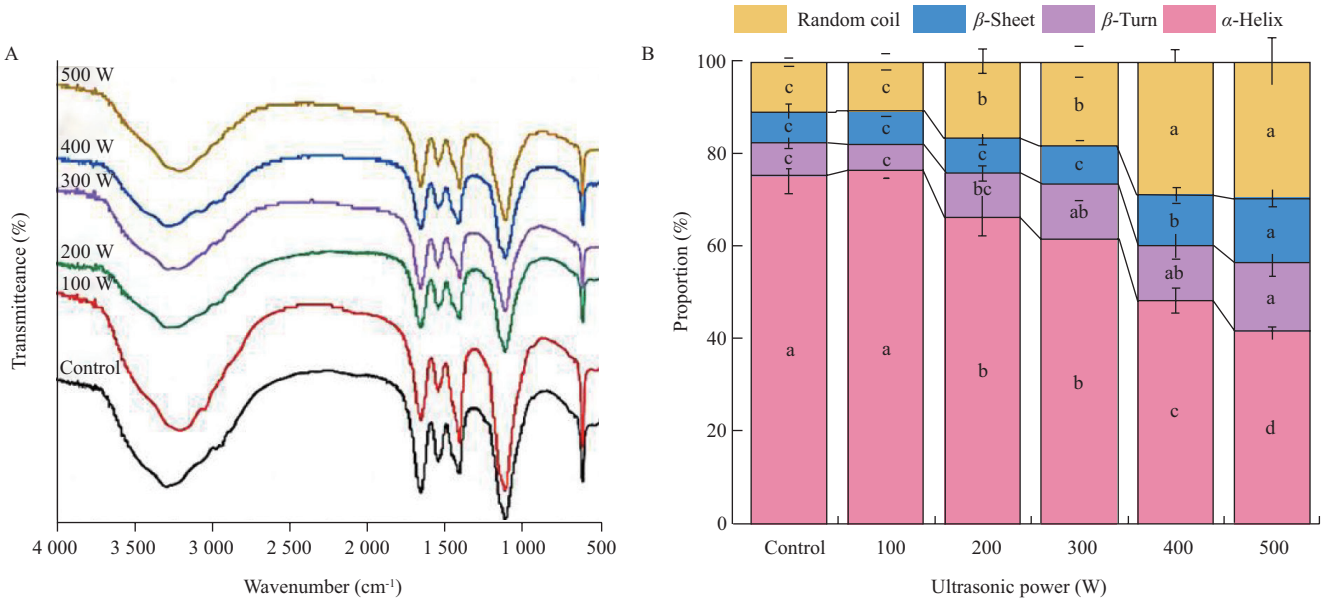

Fig. 2 Fourier infrared spectra of TM under different high ultrasonic intensity treatments (A) and the secondary structure proportion (B) of control and HIU treated TM. Different letters for means (n = 3) in the different column for same index indicate significant differences (P < 0.05).

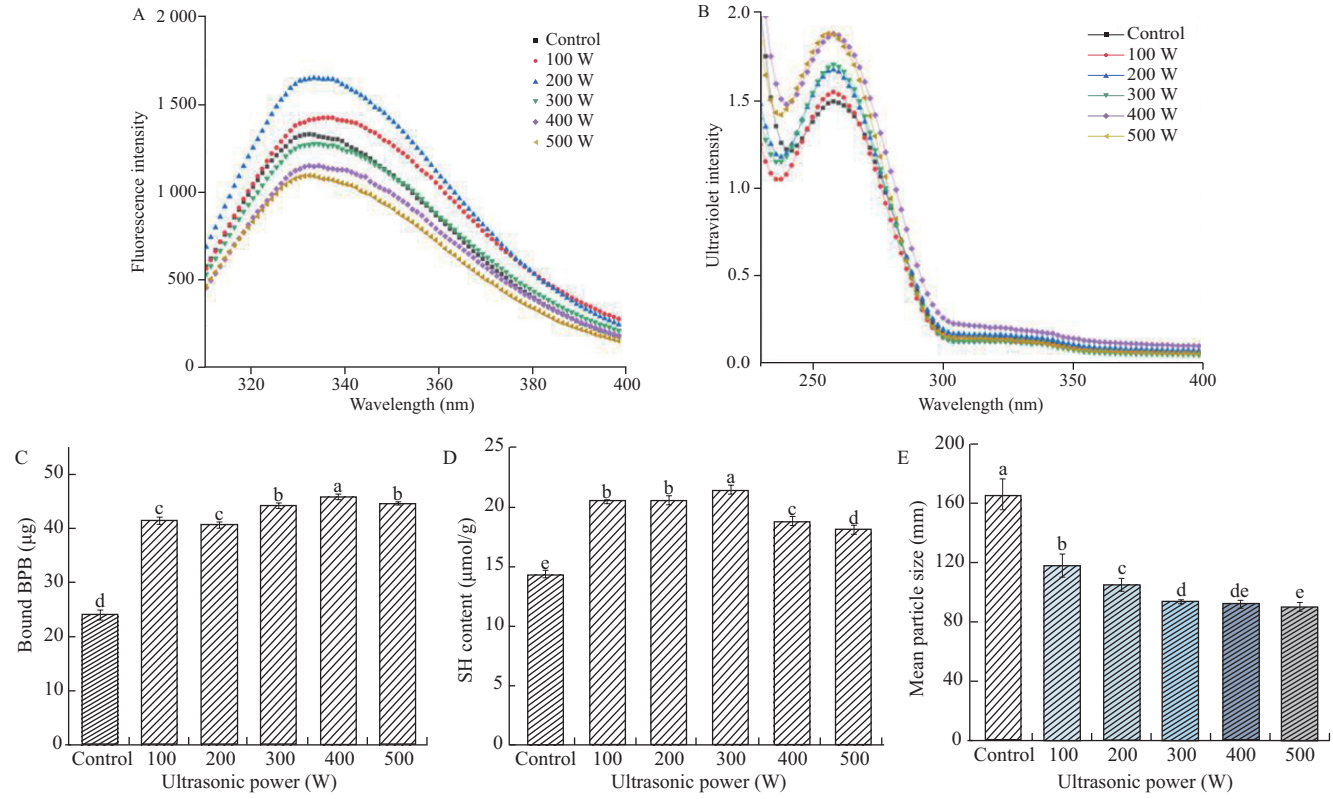

Fig. 3 Surface hydrophobicity (A), SH group content (B), intrinsic fluorescence spectra (C), and UV spectra (D), and particle size (E) of control and HIU treated TM. Mean value (n = 3) with different letters means significantly different (P < 0.05).

to the disruption of the structure of the protein molecule, resulting in the exposure of SH groups within the protein. Besides, ultrasonic treatment can excite the water molecules in solution and form free radicals[26]. This may cause oxidative modification of the sensitive SH groups to form disulfide bonds, leading to a decrease in the SH content of TM at higher ultrasonic power (> 300 W). The above results indicated that the HIU treatment method caused significant damage to the secondary and tertiary structure of TM. The unfolding and loosening of the protein affected the conformational epitopes. Therefore, HIU might affect the sensitization of TM to a great extent.

3.5 Intrinsic fluorescence spectra

The intrinsic fluorescence spectra of TM under different HIU treatments were used to further characterize the conformational changes (Fig. 3A). The results indicated that the fluorescence peak of the untreated TM was at approximately 333 nm (1 334 au). Noticeably, the maximum fluorescence intensity of the TM exhibited an increasing and then decreasing trend with HIU treatment, which was lowest for the TM treated with 500 W HIU. The maximum value was reached at an HIU power of 300 W and accompanied by a slight red shift (333−337 nm). Similar results were discovered in the effect of ultrasonic treatment on the structure of scallop sleeve membrane proteins[22]. Increased exposure of chromophores to the external environment caused the fluorescence intensity to be quenched by polar solvents, resulting in a decrease in fluorescence intensity[27]. Meanwhile, this explanation was imprinted with the enhancement of surface hydrophobicity. Moreover, the red-shift phenomenon confirmed the alteration of the microenvironment of aromatic amino acid residues induced by HIU treatment.

3.6 UV spectra

The main regions of the UV absorption peaks of TMs from different HIU treatments were consistent (250−300 nm), suggesting that aromatic amino acids determined the position of the UV absorption spectra (Fig. 3B). The peak intensity at the maximum absorption peak increased obviously with the increase of HIU power, while the peak position remained unshifted. HIU increased UV absorption through disruption of protein particles and intermolecular forces[28]. This result meant that the protein structure was unfolded by the HIU treatment, exposing more aromatic amino acid residues and leading to increased UV absorption.

3.7 Particle size

The mean particle size of the untreated and HIU-treated TM samples was shown in Fig. 3E. The mean particle size of TM significantly ($P < 0.05$) decreased with increasing HIU power, from the initial (165.5 ± 3.7) to (85.6 ± 1.8) nm. A study demonstrated that high-intensity HIU treatment resulted in the formation of granular colloids of casein with a diameter of less than 100 nm, which was consistent with the results of the present study[29]. The decrease in the mean protein particle size may be attributed to the reduction of protein aggregates after HIU treatment, which contributed to a more uniform TM dispersion and was confirmed by the AFM images.

3.8 AFM

The AFM images showed the differences in particle size, distribution, and morphology between natural and HIU-treated (500 W) TM samples at the molecular level. As depicted in Fig. 4, The protein particles of untreated TM were large with smooth edges, uneven distribution, and obvious aggregation. HIU treatment decomposes TM into small molecules with irregular edges through high-intensity dispersion, leading to an increase in surface roughness and a decrease in aggregation[30]. This result provided support for the reduction in the mean particle size of the HIU-treated TM.

3.9 IgG binding capacity analysis

To investigate the effect of HIU treatment on TM IgG binding capacity, Western blotting, dot blotting, and indirect ELISA analysis were performed using TM rabbit antiserum. The Western blotting results suggested that the immunoblot intensity of TM remained almost parallel in the range of 100−300 W, but decreased slightly at 400 W (Fig. 5A). In addition, a marked decrease in IgG immunoblot intensity was observed in the sample treated with the maximum ultrasound power (500 W). A similar trend was shown in the dot blotting results of TM samples treated with different ultrasound powers (Fig. 5B). When the ultrasound power was at 100−200 W, no difference in immunoblot intensity was observed between untreated and HIU-treated TM. However, the immunoblotting intensity of TM decreased with increasing ultrasound power (300−500 W). The indirect ELISA results showed that IgG binding values started to decrease ($P < 0.05$) when the ultrasound power was above 100 W with the most significant effect at 500 W (Figs. 5C and D). Therefore, high power HIU treatment effectively reduced the binding capacity of TM to IgG and had a potential to reduce sensitization.

Since the different processing leads to changes in the conformation of the allergen, which directly affects its allergenicity. The secondary structure results indicated that structures increased after HIU treatment. It has been argued that loss of the α-helix content of TM decreased and the proportion of disordered structure possibly hiding allergenic epitopes[26]. Consequently, the IgG binding capacity of HIU-treated TM decreased significantly at higher power levels. The hydrophobic groups within the TM were more exposed to the surface after HIU treatment, leading to folding of the protein structure and alteration of the tertiary structure. However, based on the fundamental role of epitope formation, the epitope of an allergen could not be located in a hydrophobic region[31]. In summary, the exposure of TM hydrophobic groups with high power HIU treatment increased and the IgG binding sites were hidden resulting in a reduced binding capacity to reduce allergenicity.

3.10 In vitro digestibility analysis

A common feature of allergenic proteins is a high resistance to gastrointestinal digestion, which results in the retention of intact binding sites that can trigger an allergic reaction[32]. Therefore, it is necessary to investigate the digestive properties of TM. The *in vitro* digestibility of TM was analyzed by SDS-PAGE.

The *in vitro* simulated digestion of control and HIU-treated TM was characterized by SDS-PAGE, including simulated gastric digestion stages (Figs. 6A-D) and simulated intestinal digestion stages (Figs. 6E-H). During gastric digestion, the intensity of untreated TM bands showed an obvious decrease after 60 min (Fig. 6A). However, the HIU-treated TM started to be digested at 30 min (100 W) and 10 min (300 and 500 W), respectively. In contrast, TM bands were digested more quickly after HIU treatment. SDS-PAGE results showed that TM bands were still present in all samples after 90 min of gastric digestion, indicating that TM was resistant to pepsin. Furthermore, no newly generated bands were observed because of the TM bands degradation and generation of small molecular (< 10 kDa), which were not visible in SDS-PAGE. During intestinal digestion,

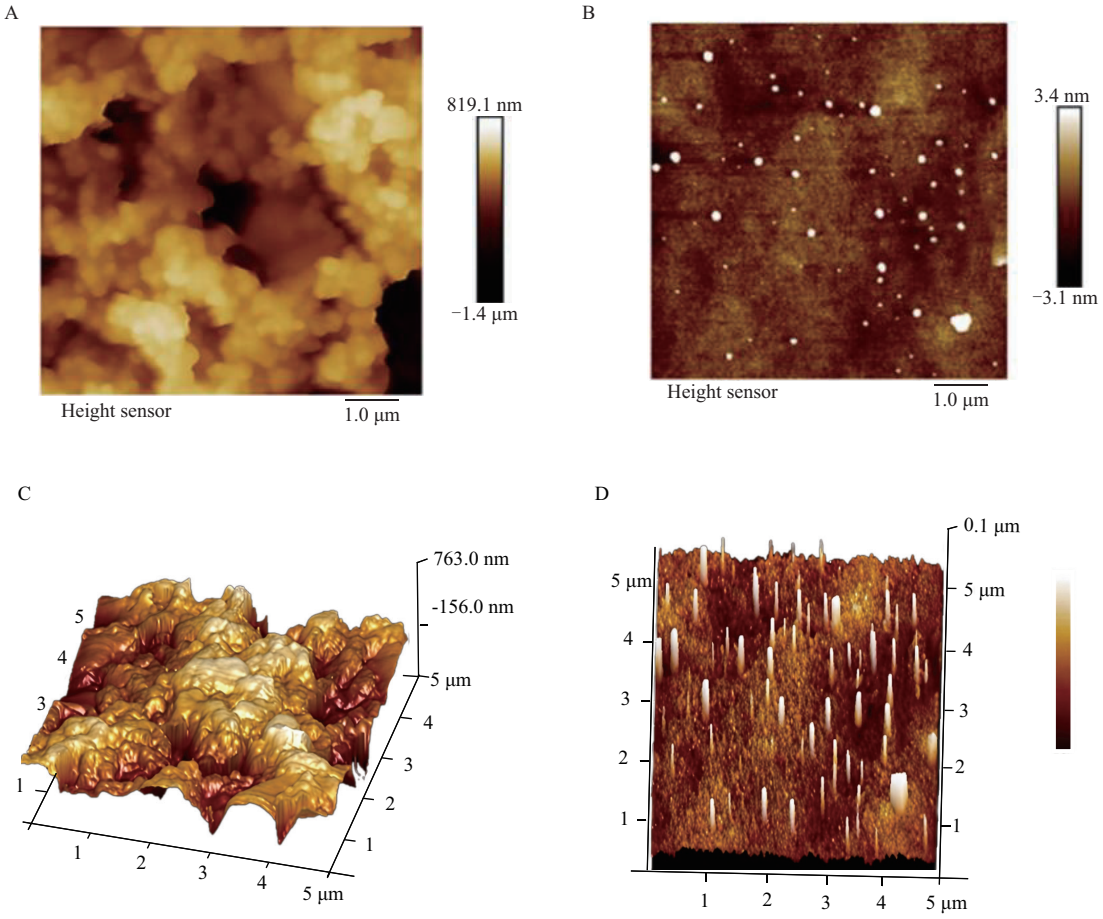

Fig. 4 AFM images of control in 2D (A) and 3D (C). TM treated with HIU at 500 W in 2D (B) and 3D AFM image (D).

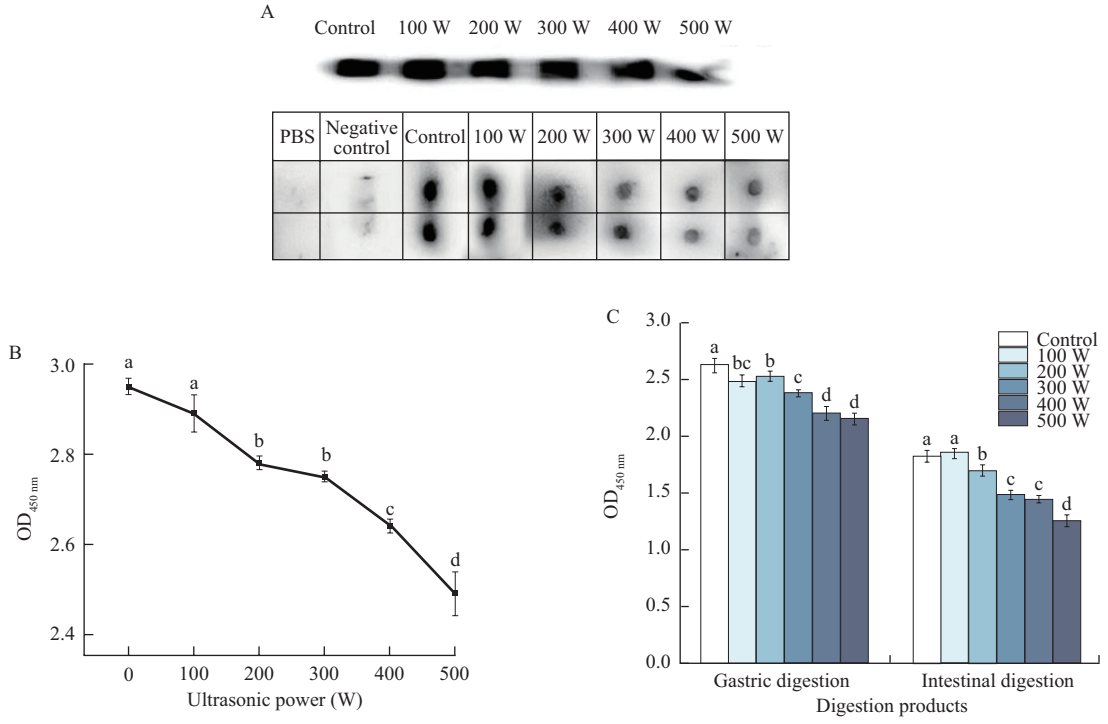

Fig. 5 Western blotting (A), dot blotting (B), indirect ELISA (C) of control and HIU treated TM, and indirect ELISA results of TM digestion products after HIU treatment (D). Mean value ($n = 3$) for same index with different letters means significantly different ($P < 0.05$).

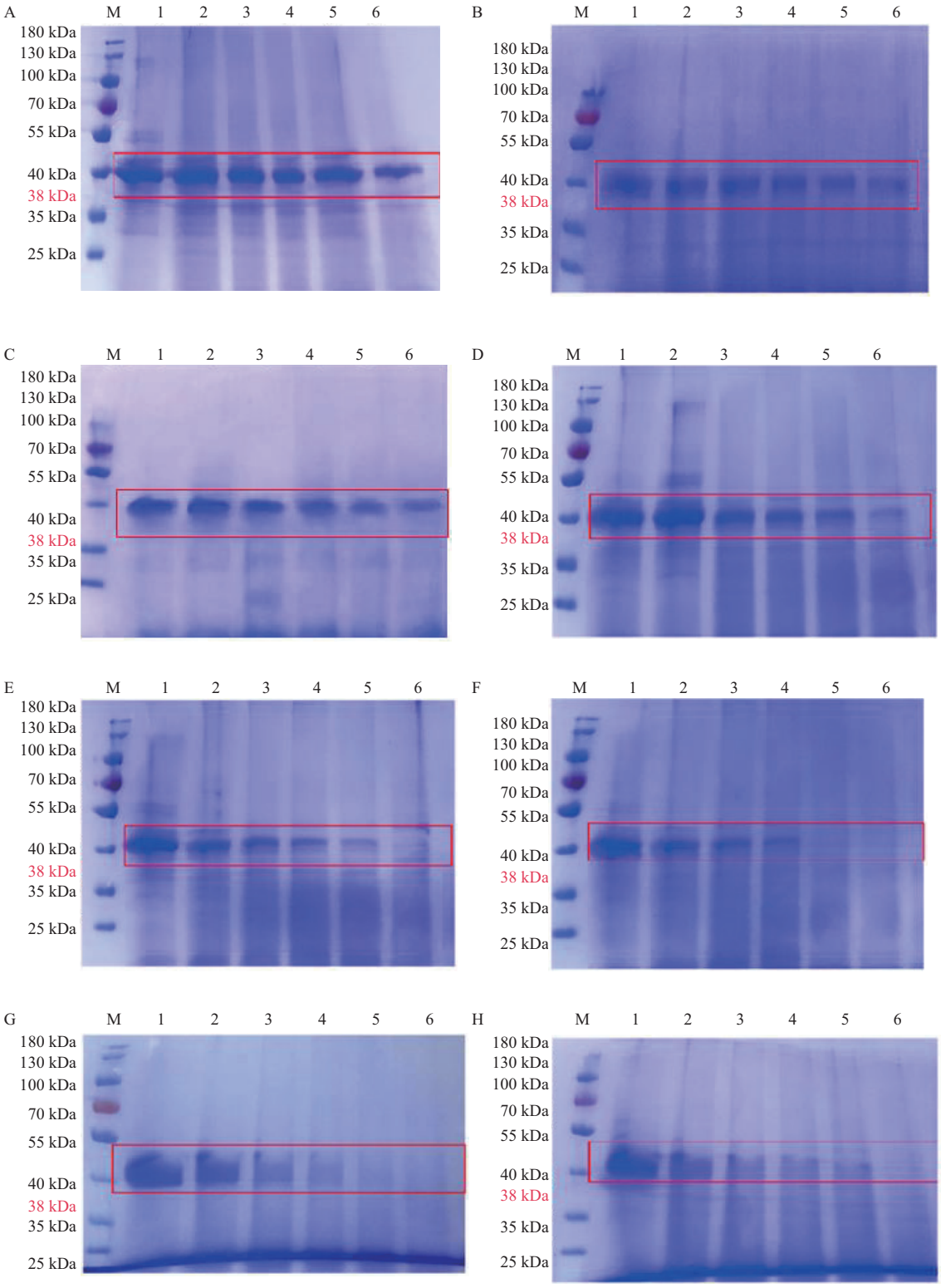

Fig. 6 Molecular weight changes of proteins during *in vitro* digestion by SDS-PAGE. Gastric stage of digestion of control (A), HIU-treated TM at 100 W (B), 300 W (C), and 500 W (D). Lane M: marker, lanes 1–6: digestion for 0, 5, 10, 30, 60, and 90 min. Intestinal digestion stage of control (E), HIU-treated TM at 100 W (F), 300 W (G), and 500 W (H). Lane M: marker, lanes 1–6: digestion for 0, 2, 5, 10, 30, and 60 min.

the intensity of untreated and HIU-treated TM bands changed appreciably with the increase of digestion time. After 60 min of intestinal digestion, the untreated TM bands were no longer visible (Fig. 6E). Moreover, the bands from 100 and 300 W treated TM disappeared at 30 and 10 min, respectively. As presented in Fig. 6H, the TM bands from samples treated at 500 W disappeared after only 5 min of intestinal digestion. These results indicated that HIU treatment promoted the *in vitro* digestibility of TM. This result was attributed to the increased proportion of disordered structures of TM induced by HIU treatment, which led to protein unfolding and exposed more enzymatic hydrolysis sites[33]. The structural change provided more recognition opportunities for the digestive enzymes and facilitated the binding of the enzymes to the substrate[8]. Additionally, the decrease in particle size of TM accelerated the penetration of digestive enzymes and improved the efficiency of enzymatic hydrolysis. The difference between gastric and intestinal digestion was related to the specificity of enzyme hydrolysis[34]. The cleavage site of pepsin was phenylalanine or tyrosine, while the site of trypsin was lysine and arginine[35]. A study proved that TM was low in phenylalanine and tyrosine but has high content of lysine and arginine[36]. Therefore, TM was more easily hydrolyzed by trypsin. The binding capacity with IgG of different HIU-treated TM digests to was further investigated by using an indirect ELISA. For untreated TM, the IgG binding abilities of TM were decreased after gastrointestinal digestion, particularly, a larger reduction was detected in the intestinal digestive products (Fig. 5D). This showed that some IgG binding epitopes of TM could be hydrolyzed by digestive enzymes. The digestion products of HIU-treated TM showed lower IgG binding values compared to the control group, reaching the lowest value (1.31) at 500 W. These results revealed that HIU treatment reduced the IgG binding capacity of TM by increasing the digestibility.

Notably, the digestion products of the TM retained IgG binding capacity even when treated at maximum ultrasound power (500 W). This meant that IgG binding sites were still present in the digested fragments, and HIU treatment could not completely eliminate the antibody recognition of TM. Although it was not possible to completely eliminate the immunoreactivity of oyster TM by HIU treatment at present, minimization of the excitation threshold could be achieved by optimizing the treatment conditions (power, time, temperature, etc.) or combined treatment. Therefore, high-power HIU treatment, as a non-thermal processing technique without destroying food quality and nutrition, can be considered as a potential strategy for reducing the allergenicity of oysters and the products.

4. Conclusion

After high intensity HIU treatment (≥ 200 W), the IgG binding capacity of oyster TM decreased in this study. The secondary structure mainly exhibited a decrease in α-helices and an increase in β-sheets and random coils. The internal hydrophobic groups of TM were exposed, proteins were unfolded, particle size was reduced, and aggregation state was altered after HIU treatment. HIU improved digestibility and reduced immune-binding activity by inducing conformational changes in TM and TM aggregates, which led to the exposure of the pepsin and trypsin cleavage sites. Indirect enzyme-linked immunosorbent results indicated lower IgG binding values for HIU-treated TM digestion products. Stronger HIU could loosen the structure of TM, reduce the immune-binding activity of TM, enhance the gastrointestinal digestibility of TM and obtain hypoallergenic digested products. High intensity HIU treatment has the potential to be an effective method for decreasing oyster allergenicity by reduction of immune binding activity of allergenic proteins.

Declaration of interests

The authors declare that they have no known competing financial interests or personal relationships that could have appeared to influence the work reported in this paper.

Acknowledgements

This work was supported by the National Key R&D Program of China (2018YFD0901005).

References

[1] J.H. Cheng, H. Wang, D.W. Sun, An overview of tropomyosin as an important seafood allergen: structure, cross-reactivity, epitopes, allergenicity, and processing modifications, Compr. Rev. Food Sci. Food Saf. 21 (2022) 127-147. https://doi.org/10.1111/1541-4337.12889.

[2] S. Aggarwal, Food allergy and food intolerance, in: Nutritional Science and Technology: Concept to Application, Scrivener Publishing LLC, 2023, pp. 317-334. https://doi.org/10.1002/9781394229116.ch14.

[3] S. Li, K.H. Chu, C.Y. Wai, et al., Genomics of shrimp allergens and beyond, Genes 14 (2023) 2145. https://doi.org/10.3390/genes14122145.

[4] Y. Lu, H. Cheng, S. Jiang, et al., Impact of three different processing methods on the digestibility and allergenicity of Chinese mitten crab (*Eriocheir sinensis*) tropomyosin, Food Sci. Hum. Wellness 12 (2023) 903-911. https://doi.org/10.1016/j.fshw.2022.09.024.

[5] T. Li, G. Bu, G. Xi, et al., Effects of heat treatment on the antigenicity, antigen epitopes, and structural properties of β-conglycinin, Food Chem. 346 (2021) 128962. https://doi.org/10.1016/j.foodchem.2020.128962.

[6] S. Yuan, C. Li, Y. Zhang, et al., Ultrasound as an emerging technology for the elimination of chemical contaminants in food: a review, Trends Food Sci. Technol. 109 (2021) 374-385. https://doi.org/10.1016/j.tifs.2021.01.048.

[7] K. Kerboua, D. Mazouz, I. Hasaounia, et al., mechanical technologies: ultrasound and cavitation in food processing, in: A. Režek Jambrak (Ed.), Nonthermal Processing in Agri-Food-Bio Sciences, Springer, Cham, 2022, pp. 1-19. https://doi.org/10.1007/978-3-030-92415-7_6.

[8] Z.F. Bhat, J.D. Morton, S. Kumar, et al., Ultrasonication as an emerging technology for processing of animal-derived foods: a focus on *in vitro* protein digestibility, Trends Food Sci. Technol. 124 (2022) 309-322. https://doi.org/10.1016/j.tifs.2022.04.012.

[9] X. Dong, J. Wang, V. Raghavan, et al., Effects of high-intensity ultrasound processing on the physiochemical and allergenic properties of shrimp, Innov. Food Sci. Emerg. Technol. 65 (2020) 102441. https://doi.org/10.1016/j.ifset.2020.102441.

[10] Y. Chen, G. Tian, L. Wang, et al., Effects of ultrasound-assisted high temperature-pressure treatment on the structure and allergenicity of tropomyosin from clam (*Mactra veneriformis*), Food Chem. X 18 (2023) 100740. https://doi.org/10.1016/j.fochx.2023.100740.

[11] M. Hussain, M.A. Gantumur, M.F. Manzoor, et al., Sustainable emerging high-intensity sonication processing to enhance the protein bioactivity and bioavailability: an updated review, Ultrason. Sonochem. 97 (2023) 106464. https://doi.org/10.1016/j.ultsonch.2023.106464.

[12] A.D. Kerezsi, N. Jacquet, C. Blecker, et al., Advances on physical treatments for soy allergens reduction - a review, Trends Food Sci. Technol. 122 (2022) 24-39. https://doi.org/10.1016/j.tifs.2022.02.007.

[13] X. Liu, Y. Ma, L. Liu, et al., Effects of high hydrostatic pressure on conformation and IgG binding capacity of tropomyosin in Pacific oyster (*Crassostrea gigas*), Food Chem. 404 (2023) 134595. https://doi.org/10.1016/j.foodchem.2022.134595.

[14] Z. Zhang, X. Zhang, W. Chen, et al., Conformation stability, *in vitro* digestibility and allergenicity of tropomyosin from shrimp (*Exopalaemon modestus*) as affected by high intensity ultrasound, Food Chem. 245 (2018) 997-1009. https://doi.org/10.1016/j.foodchem.2017.11.072.

[15] Z. Yu, Y. Wang, Z. Li, et al., Development of ELISA method for detecting crustacean major allergen tropomyosin in processed food samples, Food Anal. Methods 12 (2019) 2719-2729. https://doi.org/10.1007/s12161-019-01627-z.

[16] Z.W. Liu, L.J. Liu, Y.X. Zhou, et al., Dielectric-barrier discharge (DBD) plasma treatment reduces IgG binding capacity of β-lactoglobulin by inducing structural changes, Food Chem. 358 (2021) 129821. https://doi.org/10.1016/j.foodchem.2021.129821.

[17] R. Wang, S. Jiang, Y. Li, et al., Effects of high pressure modification on conformation and digestibility properties of oyster protein, Molecules 24 (2019) 3273. https://doi.org/10.3390/molecules24183273.

[18] Y. Zhao, Y. Yuan, X. Yuan, et al., Physicochemical, conformational and functional changes of quinoa protein affected by high-pressure homogenization, LWT-Food Sci. Technol. 173 (2023) 114343. https://doi.org/10.1016/j.lwt.2022.114343.

[19] Y. Yin, M. Jiang, Y. Liang, et al., Ultrasound improves the digestibility of oxidized silver carp (*Hypophthalmichthys molitrix*) myofibrillar protein: changes from structure to peptide release, Food Res. Int. 204 (2025) 115962. https://doi.org/10.1016/j.foodres.2025.115962.

[20] R. Mozafarpour, A. Koocheki, T. Nicolai, et al., Modification of grass pea protein isolate (*Lathyrus sativus* L.) using high intensity ultrasound treatment: structure and functional properties, Food Res. Int. 158 (2022) 111520. https://doi.org/10.1016/j.foodres.2022.111520.

[21] C.V.R.K. Tammineedi, R. Choudhary, G.C. Perez-Alvarado, et al., Determining the effect of UV-C, high intensity ultrasound and nonthermal atmospheric plasma treatments on reducing the allergenicity of α-casein and whey proteins, LWT-Food Sci. Technol. 54 (2013) 35-41. https://doi.org/10.1016/j.lwt.2013.05.020.

[22] Q. Ding, G. Tian, X. Wang, et al., Effect of ultrasonic treatment on the structure and functional properties of mantle proteins from scallops (*Patinopecten yessoensis*), Ultrason. Sonochem. 79 (2021) 105770. https://doi.org/10.1016/j.ultsonch.2021.105770.

[23] L. Kaur, B. Mao, A. S. Beniwal, et al., Alternative proteins *vs* animal proteins: the influence of structure and processing on their gastro-small intestinal digestion, Trends Food Sci. Technol. 122 (2022) 275-286. https://doi.org/10.1016/j.tifs.2022.02.021.

[24] Y. Song, Z. Li, H. Lin, et al., Effect of malondialdehyde treatment on the IgE binding capacity and conformational structure of shrimp tropomyosin, Food Chem. 175 (2015) 374-380. https://doi.org/10.1016/j.foodchem.2014.12.001.

[25] F. Zhang, S. Jiang, X. Feng, et al., Effect of heat treatment on physicochemical state and *in vitro* digestion of salt-soluble protein from Pacific oyster (*Crassostrea gigas*), LWT-Food Sci. Technol. 134 (2020) 110126. https://doi.org/10.1016/j.lwt.2020.110126.

[26] J. Zhao, Y. Li, L. Xu, et al., Insight into IgG/IgE binding ability, in vitro digestibility and structural changes of shrimp (*Litopenaeus vannamei*) soluble extracts with thermal processing, Food Chem. 381 (2022) 132177. https://doi.org/10.1016/j.foodchem.2022.132177.

[27] N. N. Mohd Yusof Chan, A. Idris, Z. H. Zainal Abidin, et al., Intramolecular charge transfer-induced solvatochromism and large Stokes shifts of furocoumarins, Mater. Chem. Phys. 276 (2022) 125406. https://doi.org/10.1016/j.matchemphys.2021.125406.

[28] R. Li, Y.L. Xiong, Ultrasound-induced structural modification and thermal properties of oat protein, LWT-Food Sci. Technol. 149 (2021) 111861. https://doi.org/10.1016/j.lwt.2021.111861.

[29] C. Wang, Q. Xie, Y. Wang, et al., Effect of ultrasound treatment on allergenicity reduction of milk casein *via* colloid formation, J. Agric. Food Chem. 68 (2020) 4678-4686. https://doi.org/10.1021/acs.jafc.9b08245.

[30] F. Geng, Y. Xie, Y. Wang, et al., Depolymerization of chicken egg yolk granules induced by high-intensity ultrasound, Food Chem. 354 (2021) 129580. https://doi.org/10.1016/j.foodchem.2021.129580.

[31] H. Lin, Z. Li, H. Lin, et al., Effect of pH shifts on IgE-binding capacity and conformational structure of tropomyosin from short-neck clam (*Ruditapes philippinarum*), Food Chem. 188 (2015) 248-255. https://doi.org/10.1016/j.foodchem.2015.05.007.

[32] B. Keshavarz, Q. Rao, X. Jiang, et al., Immunochemical analysis of pepsin-digested fish tropomyosin, Food Control 118 (2020) 107427. https://doi.org/10.1016/j.foodcont.2020.107427.

[33] L. Sun, Y. Wang, M. Miao, et al., Inhibition of α-amylase by polyphenolic compounds: substrate digestion, binding interactions and nutritional intervention, Trends Food Sci. Technol. 104 (2020) 190-207. https://doi.org/10.1016/j.tifs.2020.08.003.

[34] L. Lyu, S. Tian, I. Ahmed, et al., Effect of laccase-catalyzed cross-linking on the structure and allergenicity of *Paralichthys olivaceus* parvalbumin mediated by propyl gallate, Food Chem. 297 (2019) 124972. https://doi.org/10.1016/j.foodchem.2019.124972.

[35] Z.F. Bhat, J.D. Morton, A.E.D.A. Bekhit, et al., Emerging processing technologies for improved digestibility of muscle proteins, Trends Food Sci. Technol. 110 (2021) 226-239. https://doi.org/10.1016/j.tifs.2021.02.010.

[36] Y. Jin, Y. Deng, B. Qian, et al., Allergenic response to squid (*Todarodes pacificus*) tropomyosin Tod p1 structure modifications induced by high hydrostatic pressure, Food Chem. Toxicol. 76 (2015) 86-93. https://doi.org/10.1016/j.fct.2014.12.002.